Pillarburst proneness due to large-scale excavations in deep mines (Case study: The Provence coal mine)

S. Ahmed, Marwan Al Heib, Yann Gunzburger, Vincent Renaud

Pillarburst proneness due to large-scale excavations in deep mines (Case study: The Provence coal mine)

Ahmed, S.
Faculty of engineering- Cairo University, Cairo, Egypt
AlHeib, M.
INERIS, Nancy, France
Gunzburger, Y.
Ecole des Mines de Nancy, Nancy, France
Renaud, V.
INERIS, Nancy, France

This paper was prepared for presentation at the 53rd US Rock Mechanics/Geomechanics Symposium held in New York, NY, USA, 23–26 June 2019. This paper was selected for presentation at the symposium by an ARMA Technical Program Committee based on a technical and critical review of the paper by a minimum of two technical reviewers. The material, as presented, does not necessarily reflect any position of ARMA, its officers, or members. Electronic reproduction, distribution, or storage of any part of this paper for commercial purposes without the written consent of ARMA is prohibited. Permission to reproduce in print is restricted to an abstract of not more than 200 words; illustrations may not be copied. The abstract must contain conspicuous acknowledgement of where and by whom the paper was presented.

ABSTRACT: The objective of this paper is to examine the applicability of the rockburst proneness criteria by using the numerical modeling tool. Many rockburst criteria are illustrated by the case of a deep coal mine in France, in which pillarburst (RC2) took place in 1993 in the shaft station, which is located at 1000 m from the earth's surface and it was excavated in 1984 by using the room-and-pillar mining method. The shaft station is surrounded by several longwall panels that were exploited between 1984 and 1994. To assess the stress redistribution and the stored strain energy concentration due to mining operations, a detailed large-scale finite difference numerical model of the mine has been constructed. The excavations in the numerical model are performed into two steps. Firstly, the shaft station galleries' are excavated to determine their effect on the bursted pillar (RC2). Then, the longwall panels are excavated year by year to detect their effect on the shaft station pillars'. The numerical modeling results show that the vertical stress increased on the pillars due to the excavation of the longwall panels. To assess the pillarburst proneness in the shaft station area, the energy-based rockburst criteria (i.e., Loading System Stiffness (*LSS*)) are found to be more efficient than the stress-based rockburst criteria (i.e., Brittleness coefficient (B)).

1. INTRODUCTION

The most probable underground instability during the room-and-pillar mining is the pillar failure (Zipf, 2001). Two major types of pillar failures are identified; i) the structurally controlled failure; and ii) the progressive failure. The structurally controlled failure occurs when a rockmass contains planes of failure (i.e., discontinuities) and the pillars are oriented unfavorably with respect to those planes of failure. This type of failure could be easily observed. The progressive failure takes place where the pillar skin has high vertical stress and little horizontal confinement. Initially the pillar remains intact and retains its bearing capacity, then, as the spalling takes place, the stresses are redistributed and reached up to the pillar core progressively until it reaches a critical cross-section area and fails. This failure could occur in a violent brittle manner, which is called pillar-burst (type of rockburst).

The Factor of Safety (F.S = pillar strength/average pillar stress) is usually used to assess pillars stability and its failure tendency. Many authors developed empirical formulas to assess coal pillar strength. For example, Salamon and Munro, 1967 studied 125 pillars in the South African coal fields and they developed Eq. (1) to assess the coal pillar strength.

$$\sigma_{ps} = \mathrm{K}\left(\frac{\mathrm{w}^{\mathrm{b}}}{\mathrm{h}^{\mathrm{a}}}\right) \quad (1)$$

Where K is the strength of a unit cube of coal (7.2 MPa), σ_{ps} is the pillar strength (MPa), w is the pillar width, h is the pillar height, a and b are empirical constants, where a = 0.66 and b = 0.46.

However, the Factor of Safety is found to be insufficient to express the pillars instability in case of mines with complex geometry, where pillars have irregular shapes and volumes. To predict the rockburst hazard, many criteria have been developed to assess the rockburst proneness in underground mines. Some of those criteria are based on the intact rock mechanical properties that are obtained from uniaxial laboratory tests. Other criteria are based on the in-situ induced stresses and the elastic energy stored in rock due to mining operations. However, the influence of each parameter on the rockburst occurrence

has never been tested. Some of the rockburst criteria are presented below:

1.1. Brittleness coefficient (B)

Peng and Wang, 1996 carried out an experimental study to estimate the rockburst proneness by using the brittleness coefficient (*B*), which is independent of the in-situ stress field. The *B* coefficient is equal to the ratio between the uniaxial compressive strength (σ_c) and the tensile strength (σ_t) as shown in Eq. (2).

$$B = \frac{\sigma_c}{\sigma_t} \tag{2}$$

Where σ_c and σ_t are the compressive strength and the tensile strength of rock, respectively. The rockburst proneness has been classified according to the *B* value as follows:

(i) No rockburst: $B > 40$.
(ii) Weak rockburst: $26.7 < B \leq 40$.
(iii) Moderate rockburst: $14.5 \leq B \leq 26.7$.
(iv) Strong rockburst: $B < 14.5$.

1.2. Tao discriminant index (α)

Tao discriminant index (α) (Tao, 1988) is mainly based on the stress reduction factor reported in the Q-rockmass classification system developed by Barton *et al.,* 1974. Tao, 1988 suggested that his discriminant index could be calculated as follows (Eq. (3)):

$$\alpha = \frac{\sigma_c}{\sigma_1} \tag{3}$$

Where σ_1 is the maximum in-situ principal stress and σ_c is the unconfined compressive strength. The rockburst proneness is classified according to Tao index as follows:

(i) No rockburst: $\alpha > 14.5$.
(ii) Weak rockburst: $5.5 < \alpha \leq 14.5$.
(iii) Moderate rockburst: $2.5 \leq \alpha \leq 5.5$.
(iv) Strong rockburst: $\alpha < 2.5$.

1.3. Competency Factor (C_g)

Palmstrom, 1995 enhanced the Russenes criterion (T_s) (Russenes, 1974) by taking the rockmass scale effect into consideration. He used the Rock Mass Index (*RMi*) classification system to edit the Russenes criterion from a small-scale (i.e., laboratory scale) to a large-scale (i.e., rockmass scale). Palmstrom developed the competency factor (C_g) to assess the rockburst proneness, which could be expressed as follows (Eq. (4)):

$$C_g = \frac{RMi}{\sigma_\theta} = \frac{f_\sigma \,.\, \sigma_c}{\sigma_\theta} \tag{4}$$

Where σc is the uniaxial compressive strength of rock (MPa), σ_θ is the maximum tangential stress of surrounding rock (MPa) and f_σ is the scale effect for the uniaxial compressive strength. For 1 – 15 m^3 block size, the rockmass property $f_\sigma = 0.45 - 0.55$.

Palmstrom, 1995 classified the failures modes in brittle massive rockmass as follows:

(i) No induced instability: $C_g > 2.5$.
(ii) Slightly loosening: $C_g = 2.5 - 1$.
(iii) Light rockburst or spalling: $C_g = 1 - 0.5$.
(iv) Heavy rockburst: $C_g < 0.5$.

1.4. Loading System Stiffness (LSS)

Wiles, 2002 assessed the pillars stability in terms of their loading stages. He assumed that the pillar on its intact state is at 'Stage I' and during the loading until the burst it arrives to 'Stage II' as shown in Fig. (1). The Loading system stiffness (*LSS*) represents the slope of the load deformation response curve of the pillar loading process.

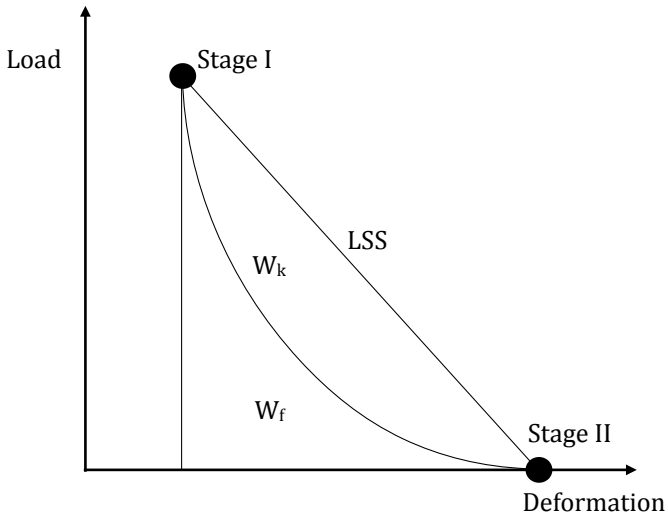

Fig. 1. Loading deformation response of pillar.

The total amount of energy released from the surrounding rockmass during pillar failure (W_r) is the area of the triangle in Fig. (1) that could be expressed as follows (Eq. (5)):

$$W_r = W_f + W_k \tag{5}$$

Where W_k is the kinetic energy and W_f is the amount of energy that would be used to crush the pillar (Wiles, 2002). He suggested that the slope between stage I and stage II (*LSS*) could be expressed in terms of mean stress (σ_m) (Eq. (6)) and volumetric strain (ε_v) (Eqs. (7 and 8)), when the post-peak behavior of the pillar material matches the behavior reported in Fig. (1). Wiles, 2002 did not provide a range of *LSS* that if we find, we would estimate the rockburst proneness. But, the rockburst proneness generally increases with decreasing of (1/LSS $=\varepsilon_v / \sigma_m$) value.

$$\sigma_m = LSS\, \varepsilon_v \tag{6}$$
$$\sigma_m = (\sigma_1 + \sigma_2 + \sigma_3)/3 \tag{7}$$
$$\varepsilon_v = (\varepsilon_1 + \varepsilon_2 + \varepsilon_3) \tag{8}$$

In the current research, different rockburst criteria are successively implemented in a large-scale numerical model of a real rockburst case study (pillarburst type) in

order to assess their applicability and their efficiency to describe the pillarburst event that took place in the shaft station area. The case study is presented in details in the next section.

2. CASE STUDY

The present case study concerns the Western part of the Provence coal mine, which is located in the South of France. It had been in operation from 1984 until 1994 using the longwall mining method as shown in Fig. (2). The average thickness (t) of the exploited coal seam is 2.5 m and it lies at depth ranges between 700 m and 1300 m (the coal seam dips 10°). The shaft station area of the mine was excavated before the longwall panels by using the room-and-pillar mining method (Fig. 2), where the galleries width is 5 m on average and the pillars have irregular dimensions. The shaft station pillars' are self-supported and the impact of the ground support has not been addressed in the current case study. The shaft station is located at depth 1000 m from the earth's surface. The overburden consists mainly of Fuvelian limestone, Begudo-Rognacian limestone, and marl as shown in Fig. (3). Below the coal seam, the rockmass contains Jurassic limestone in majority (Fig. 3). The coal seam contains a stiff limestone bed with maximum thickness 50 cm at its middle. Table 1 shows the average rockmass mechanical properties for each rock layer (Ahmed *et al.*, 2016). The rockmass properties are estimated based on laboratory tests.

On October 1993, a pillarburst of 2.7 magnitude (weak to strong rockburst on Richter scale (Bieniawski, 1987)) has been recorded in the main shaft station area in the Provence coal mine. The reported damage is limited to a single pillar, which is the smallest coal pillar in shaft area.

In this study, the numerical modeling tool is used to assess the influence of longwall panels' excavation on the adjacent shaft station pillars' in the Provence coal mine. Also, the relation between the pillar dimensions and its failure tendency is investigated. The rockburst criteria are used as useful tool to back-analyze the pillarburst proneness of the shaft station pillars', especially the pillar RC2.

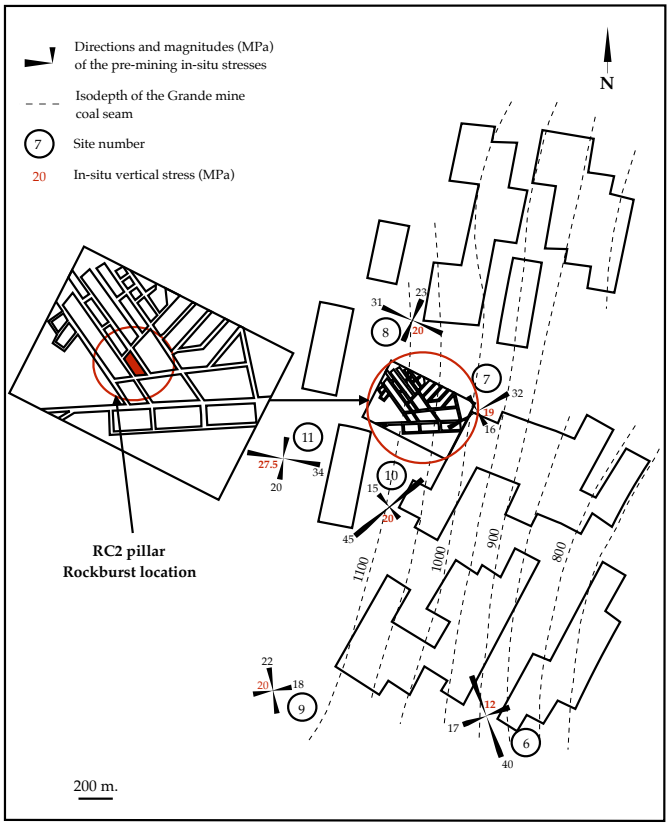

Fig. 2. Layout of the western part of the Provence coal mine – France (shaft station and longwall panels (1984-1994)).

3. NUMERICAL MODEL AND METHODOLOGY

The initial design of the shaft station considered that this area is safe and out of the rockburst hazard. To explain and understand why the pillarburst occurred in the shaft area, many analysis and investigations were performed by using 2D numerical modeling (Tinucci, 1993). However,

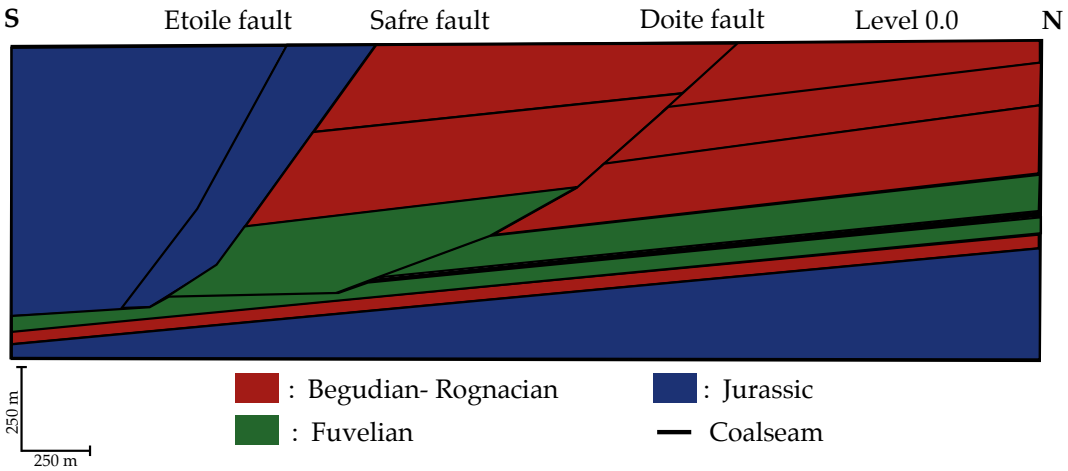

Fig. 3. Geological cross section of the mined area.

the 2D models were not able to describe efficiently the causes behind such brittle failure, because many factors were not taken into consideration such as; the third dimension, the pillar irregularity and its relevance to the surrounding pillars and panels.

To investigate the instability of the shaft station area in complete and complex manner, a 3D numerical model of the mine was constructed using the finite difference numerical method FLAC^{3D} (Fig. 4). The mesh density is adjusted to be fine close to the excavated area and it increases by ratio of 1.2 until model borders. This model contains approximately 2.5 million zones. Four different rock formations are specified: the coal seam, the Fuvelian limestone (400 m), the Rognacian limestone (600 m) above, and the Jurassic limestone below the coal seam. The overall dimensions of the model are 4600 m in the x-direction, 6020 m in the y-direction and 2270 m in the vertical direction as shown in Fig. (4).

The top of the model coincides with the ground surface at level z=0.0 (Fig. 4). The boundary conditions of the model are fixed except the top (free surface). The vertical stress within the model is equal to the overburden weight. The mechanical behavior of the model is elastic, except in the shaft station area, where the Mohr-Coulomb mechanical model is applied. Table 1 shows the mechanical properties of rock layers.

Based on the pre-mining in-situ stress measurements provided by Gaviglio *et al.*, 1996 (Fig. 2), Ahmed *et al.*, 2016 developed a methodology to initialize the stress state in the large-scale numerical models (for example, the Provence coal mine). The Simplex Method is used to calculate the linear stress gradients (g_x, g_y, and g_z) by minimizing the squared difference between the measured stresses and their numerical values. Table 2 shows the initial stress (pre-mining stress) values for all stress components at (0,0,0) and their 3D stress gradients.

After reproducing the pre-mining stress state in the numerical model, the shaft station galleries' and the longwall panels are excavated year by year. Firstly, the galleries (denoted by black color in Fig. 4b) of the shaft station are excavated to observe their influence on the adjacent coal pillars, especially the pillar RC2 (the failed pillar). Secondly, the longwall panels are excavated gradually from 1984 until 1993 to observe the stress changes numerically on the shaft station pillars'.

Table 2. Stress components used for obtaining pre-mining stresses in the numerical model, Ahmed *et al.*, 2016.

Stress (MPa) at (x=0, y=0, z=0)		Stress gradient (MPa/m)		
		g_x	g_y	g_z
σ_{xx}	-0.01	-0.001162	-0.0038	0.0166
σ_{yy}	-0.01	-0.00575	0.0033	0.0194
σ_{zz}	0.01	0.005434	-0.00168	0.0235
σ_{xy}	0.01	-0.003312	0.001162	0.0

Table 1. Average rockmass mechanical properties, Ahmed *et al.*, 2016.

Rock type	Density (kg/m^3)	$E_{rockmass}$ (MPa)	Poisson ratio	ϕ (°)	UCS (MPa)	T (MPa)	Brittleness coefficient (B)
Lignite coal	1500	2000	0.3	30	28	1	28
Limestone seam (50 cm)	2400	23000	0.1	35	80	3.17	25
Fuvelian	2400	8450	0.2	-	-	-	-
Rognacian	2400	1000	0.25	-	-	-	-
Jurassic	2400	17000	0.25	-	-	-	-

Where $E_{rockmass}$ is the rockmass deformation modulus, UCS is the unconfined compressive strength (MPa), T is the tensile strength (MPa), ϕ is the internal friction angle.

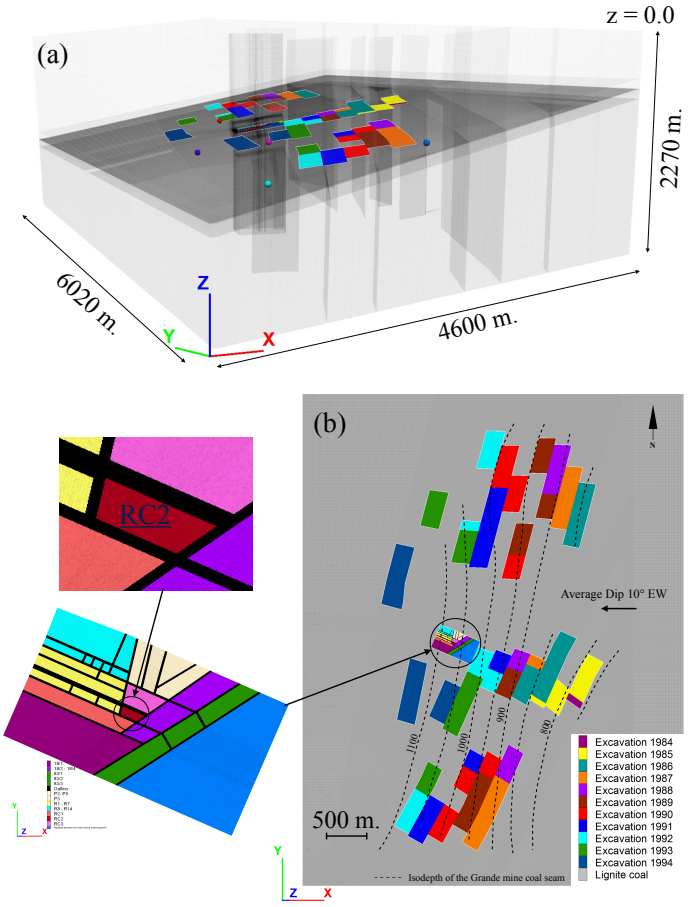

Fig. 4. The numerical model (a) 3D view of the entire model (b) Layout of the shaft station area and the panels excavated (1984 – 1994).

To assess the stability of the shaft station pillars', the volume of plastic volume at pillars skin is recognized for each pillar. Meanwhile, the four rockburst criteria; Brittleness coefficient (B), Tao discriminant index (α), Competency factor (C_g) and Loading System Stiffness (LSS) are implemented within the large-scale model to test the pillarburst tendency of the pillar RC2 and 8 of its neighbors due to panels excavations.

4. RESULTS AND DISCUSSION

After excavating the galleries then the panels, the results show that the maximal vertical stress increased by 1.5 times its pre-mining value (Fig 5). We also noticed that, after galleries excavation, the vertical stress increment concentrated at the pillars edges as shown in Fig. 5a. However, after excavating the longwall panels, at the end of 1993 (the year of the pillarburst) the vertical stress increment extended up to the pillar cores, especially in the pillar RC2 as shown in Fig. 5b.

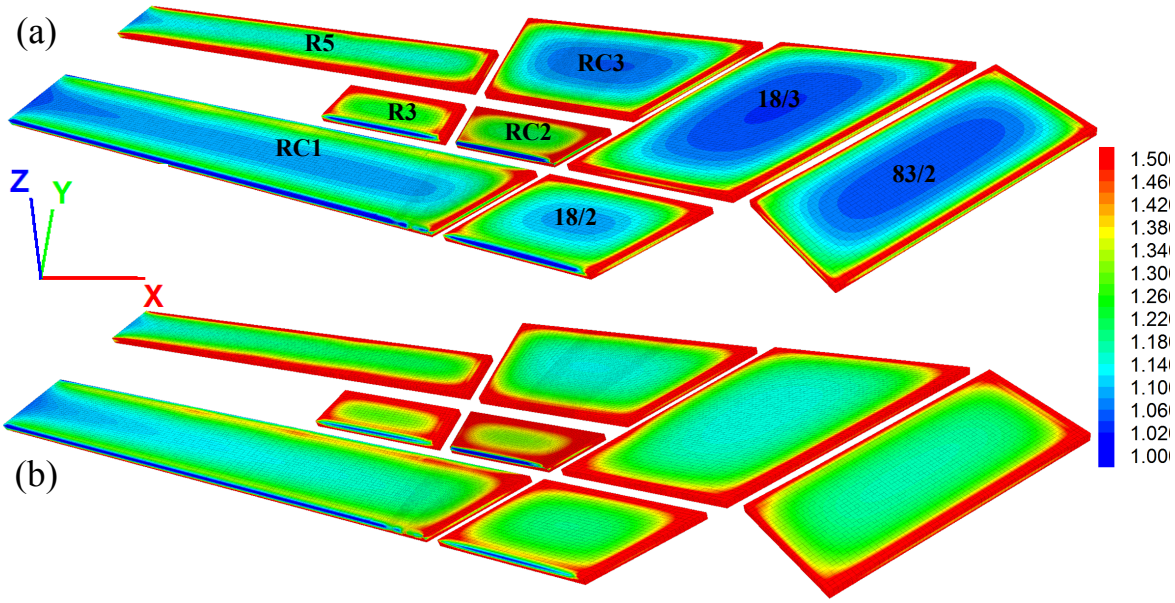

Fig. 5. Normalized vertical stress distribution ($\sigma_{zz}/\sigma_{zz(ini)}$) (a) after excavation of shaft station galleries (b) after panels excavation in 1993.

The main question is how these stress changes could lead to the pillarburst of RC2? The elastic-perfect plastic mechanical behavior (Mohr-Coulomb) is used for the coal pillars and strain-softening mechanical behavior, which simulates degradation of the resistance in function of the plastic deformation, is implemented on the limestone seam at the middle of the coal pillars. The elastic-perfect plastic calculation is performed to recognize the effect of panels' excavation in terms of plastic volume per pillar volume. We noticed that the smallest pillar (RC2) gained the highest percentage of plastic strain at its edges due to excavations (Fig. 6), where 30% of the pillar exposed to plastic deformation. And, the largest pillar (RC1) gained the lowest percentage of plastic volume at its edge. Furthermore, we found that the percentage of plastic volume did not increase due to the excavation of the longwall panels as shown in Fig. (6). The plastic volume were kept almost constant after excavating the shaft station galleries' and the longwall panels' (at the end of 1993). We also noticed that, the shear yield was the dominant failure mode and the tension failure appeared at the level of stiff limestone seam, but, it did not extend up to the pillar core as shown in Fig. (6).

As shown in Fig. (5), due to longwall panels' exploitation, the stress increment reached up to the pillar cores, which could threaten their stability. The strength of RC2 pillar ($\sigma_{ps} = 14$ MPa**)** could be estimated from Eq. (1) (w = 17.5 m, h = 2.5 m). The pillar strength is very low compared to its average stress (30 MPa).

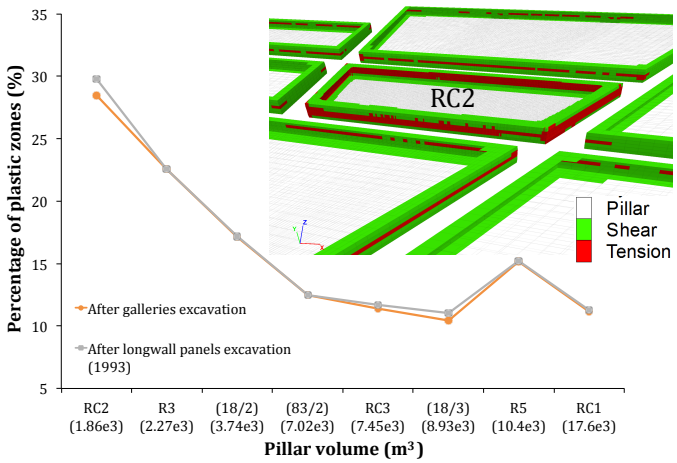

Fig. 6. Shear and tension plastic volume (%) on shaft station pillars.

However, the elastic-perfect plastic mechanical behavior was not able to describe sufficiently this difference between the pillar average stress and its strength in terms

of plastic failure. For that, four different rockburst criteria were implemented in the numerical model as a useful tool to explain the stress changes in terms of failure tendency.

The results show that the brittleness coefficient (B) criterion gives a constant value across all the shaft station pillars. The B value is found to be equal to 28 for the coal seam and 25 for the Limestone seam as shown in Table 1. These B values announce moderate rockburst tendency. But, this type of rockburst criterion that depends only on laboratory scale mechanical properties is found to be insufficient in case of large-scale complex excavations.

Tao discriminant index (α) criterion produces a distribution similar to the maximum principal stress distribution. Tao index predicts a strong rockburst tendency ($\alpha < 2.5$) for all shaft station pillars. However, The Competency factor (C_g) distribution shows that the pillars RC2 and R3 have heavy rockburst propones (C_g <0.5) and the rest of pillars have light rockburst proneness or spalling (C_g =1 - 0.5). The Competency factor is able to distinguish the rockburst proneness between groups of pillars, but, it is not able to differentiate between the failed pillar and the other safe pillars (Fig. 7).

On the other hand, the inverse of the Loading System Stiffness (1/LSS) criterion is able to distinguish between the failed pillar and other pillars. The 1/LSS varies from pillar to another as shown in Fig. (8). The (1/LSS) is very high at the core of the pillar RC2 (the smallest pillar), while the other pillars on the shaft station have medium to small failure tendency (Fig. 8). The results obtained from the (*1/LSS*) distribution correspond the results obtained from applying the elastic-perfect plastic mechanical behavior, where the pillars RC2 and R3 gained the highest percentage of plasticity at their edges. The inverse Loading System Stiffness (1/LSS) criterion was found to be a good tool to estimate the rockburst proneness, because it is a function of the three principal stresses and three principal strains.

5. CONCLUSION

This paper presented a back analysis of a pillarburst (type of rockburst) case study based on the large-scale numerical modeling and the assessment of different rockburst criteria. We examined the pillarburst proneness at the shaft station of the Provence coal mine (France). The shaft station was excavated by using the room-and-pillar mining method, where it was surrounded by many panels that were excavated by the longwall mining method. The longwall panels were excavated during 10 years between 1984 until 1994. A stiff limestone bed was

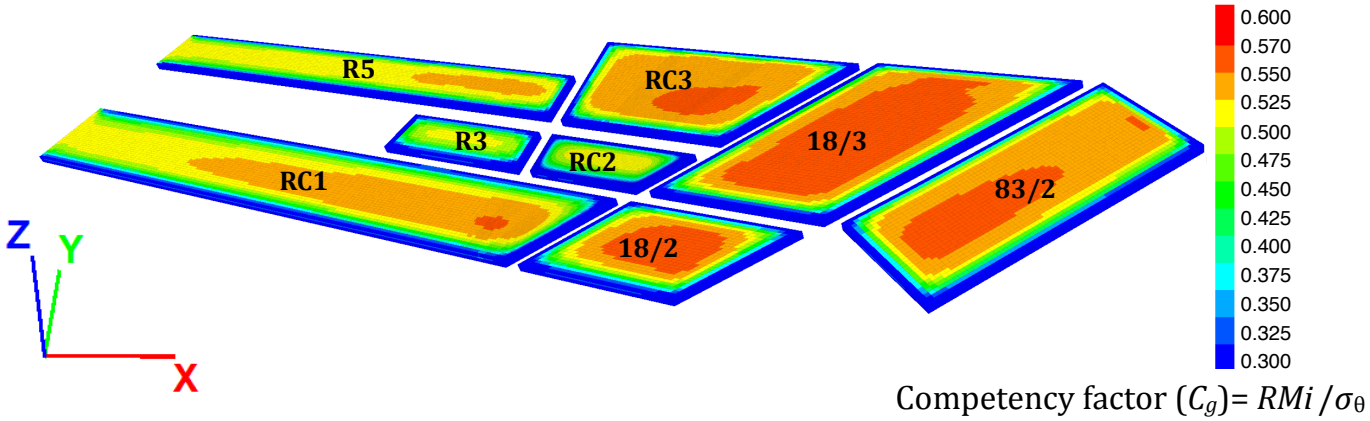

Fig. 7. Distribution of pillarburst proneness at shaft station pillars' (Competency factor (C_g) criterion).

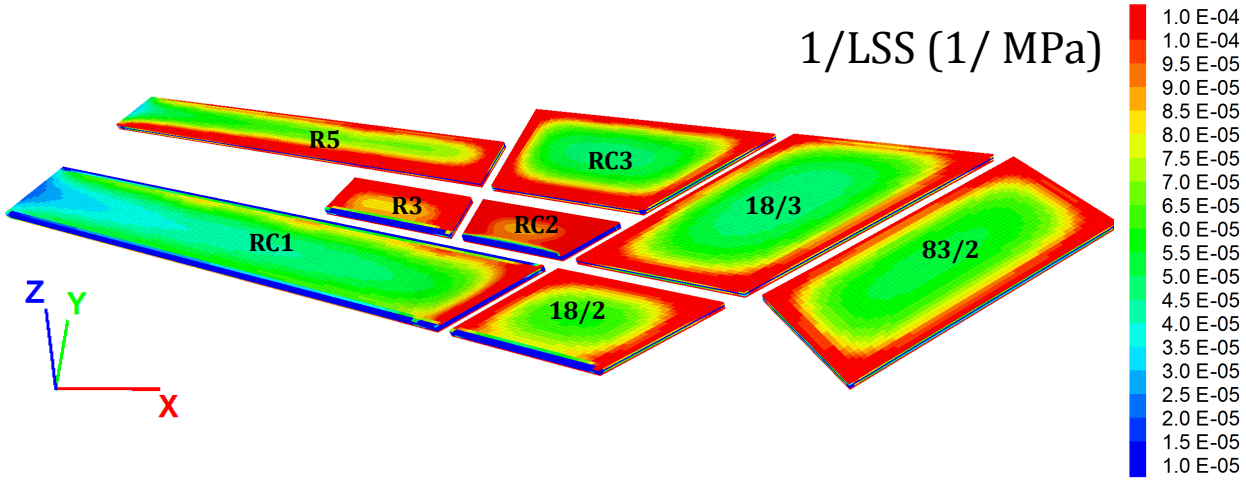

Fig. 8. Distribution of pillarburst proneness at shaft station pillars' ((1/ LSS) criterion).

recognized at the middle of the coal pillars at the shaft station area. A pillar burst was recorded in the shaft station area in 1993. A 3D numerical model was constructed to simulate the longwall panels and the shaft station area to evaluate the influence of the large-scale excavations on the pillars instability. Firstly, the shaft station galleries were excavated, then, the longwall panels were excavated.

It was found that, due to the excavation, the vertical stress increased by 1.5 times its pre-mining value. The vertical stress increment concentrated at the pillar edges after the galleries excavation. But, this stress increment extended up to the pillars cores' after longwall panels' excavation. Mohr-Coulomb mechanical criterion was used to evaluate this stress increment in terms of plastic failure. But, we noticed that the smallest pillar gained the largest percentage of plasticity and the largest pillar gained the smallest percentage of plasticity. The predominant yield type was the shear yield, and tension yield appeared at the level of the stiff limestone seam at the middle of coal pillars. However, the percentage of plastic volume did not increase due to longwall panels' excavation. For that, we concluded that the elastic-perfect plastic mechanical model is not able alone to predict the pillarburst occurrence or the pillars instability.

After implementing the rockburst criteria, it was concluded that the criterion based on the laboratory values like the Brittleness coefficient (B) gave constant rockburst tendency across all the pillars, which is not realistic and could not be applied on large-scale and complex underground excavations. Also, the criteria that are based on stress changes like Tao discriminant index (α) criterion gave rockburst tendency distribution similar to that stress distribution. However, the criteria that are based on energy changes during excavations like the inverse Loading System Stiffness ($1/LSS$) criterion gave a realistic burst tendency that corresponds to the stress and strain increment during excavations. The $1/LSS$ criterion is able to distinguish between the failed pillar and the other pillars.

More investigations are required in the Provence coal mine to observe numerically the evolution of the stored strain energy within the shaft station pillars during the panels' excavation. Also, other rockburst criteria could be implemented within the numerical model to observe their applicability in such large-scale complex excavations.

The ground support influence has not been considered in the current research as it concerns only the assessment of the rockburst criteria in a case study contains self-supported pillars. Further studies are needed to address the influence of the ground support on the pillarburst proneness.

REFERENCES

1. Ahmed S., Y. Gunzburger, V. Renaud, M. AlHeib. 2017. Initialization of highly heterogeneous virgin stress fields within the numerical modeling of large-scale mines. *Int. J. Rock Mech Min. Sci.* 99:50-62.
2. Barton N.R., R. Lien, J. Lunde. 1974. *Engineering classification of rock masses for the design of tunnel support. Rock Mech*. 6: 189–239.
3. Bieniawski Z.T. 1987. Rockburst- their mechanism and control. In *Strata control in mineral engineering*, ed. John Wiley & Sons, 135–146.
4. Gaviglio P., P. Bigarre, H. Baroudi, J.P. Piguet, R. Monteau. 1996. Measurements of natural stresses in a Provence mine (Southern France). *J. Eng. Geology*. 44: 77–92.
5. Palmstrom A. 1996. Some practical applications of the rock mass index (RMi). *Tunneling and underground space technology*. 11(3): 287–303.
6. Peng Z.H.U., Y. Wang. 1996. Griffith theory and the criteria of rock burst. *Chinese J. Rock Mech. Eng*. 17: 491–495.
7. Russenes B.F. 1974. *Analyses of Rockbursts in Tunnels in Valley Sides* [M.Sc. thesis]. Norwegian, Dept. of Geology: University of Trondheim.
8. Salamon M.D.G., A.H. Munro. 1967. A study of strength of coal pillars. *J. Sth. Afr. Inst. Min. Metal*. 68: 56–67.
9. Tao Z.Y. 1988. Support design of tunnels subjected to rockbursting. In: Romana (Ed.), *ISRM International Symposium, Rock Mechanics and Power Plants*, Madrid, Spain, September, 407–411.
10. Tinucci J.P. 1993. Analysis of pillar capacity in the vicinity of the Yvon Morandat shaft at U.E. Provence, *Itasca consulting group report to unité d'exploitation Provence*.
11. Wiles T. 2002. Loading system stiffness – A parameter to evaluate rockburst potential. *First international seminar on deep and high stress mining*. Australian center for geotechnics.
12. Zipf, R.K. 2001. Toward Pillar Design to Prevent Collapse of Room-and-Pillar Mines. 2011. *108th Annual Exhibit and Meeting, Society for Mining, Metallurgy, and Exploration, Denver, CO, 26-28 February*.